Dominance of the first excitation step for magnetic circular dichroism in near-threshold two-photon photoemission

K. Hild,* G. Schönhense, and H. J. Elmers
Institut für Physik, Johannes Gutenberg-Universität, D-55099 Mainz, Germany

T. Nakagawa and T. Yokoyama
Institute for Molecular Science, The Graduate University for Advanced Studies (Sokendai), Myodaiji-cho, Okazaki 444-8585, Japan

K. Tarafder and P. M. Oppeneer
Department of Physics and Astronomy, Uppsala University, Box 516, S-75120 Uppsala, Sweden

(Received 20 September 2011; revised manuscript received 11 January 2012; published 23 January 2012)

Magnetic circular dichroism (MCD) in near-threshold photoemission is measured for a perpendicularly magnetized Cs/Co/Pt(111) film with work function adjusted by Cs adsorption. For one-photon photoemission (1PPE) the MCD asymmetry is recorded at a fixed photon energy of $h\nu = 3.06$ eV and varying work function Φ. The asymmetry shows a nonmonotonous behavior in dependence of the excess energy $h\nu$-Φ with a maximum value of $A_{1PPE} = 6.2$ % at $\Phi = 2.45$ eV. The measurement explores the first excitation step of a former two-photon photoemission (2PPE) measurement with $A_{2PPE} = 8.4\%$ demonstrating that in 2PPE from Co(111) the first excitation step is the dominant asymmetry-generating process. An energy-dependent measurement in 2PPE at reduced work function ($\Phi \approx 3$ eV) yields a constant asymmetry of about 17% in the photon energy range between $h\nu = 1.53$–1.66 eV. It reveals that for Co(111) the involvement of a real intermediate state is crucial for enlarged MCD asymmetries. Both results are discussed in the framework of direct interband transitions in directions deviating from the direction of normal electron emission Γ-L. The 1PPE measurement is in reasonable agreement with calculations on the basis of this model. This reveals that an *ab initio* calculation considering all directions of excitation with an additional restriction in energy due to the existence of the sample work function in the photoemission process adequately describes MCD asymmetries in near-threshold photoemission.

DOI: 10.1103/PhysRevB.85.014426 PACS number(s): 75.50.Cc, 78.20.Ls, 71.20.−b, 79.60.Dp

I. INTRODUCTION

Recently, measurements on magnetic circular dichroism (MCD) in near-threshold photoemission have attracted strong interest. They prove that large magnetic asymmetries are not only associated with the regime of x-ray magnetic circular dichroism (XMCD), where discrete atomic core levels with a large spin-orbit coupling are excited.[1–3] In contrast, comparably large asymmetry values can also be detected in the near-threshold photoyield.[4–10] Experiments on perpendicularly magnetized Ni films on Cu(001) reveal MCD asymmetries $\geqslant$10% in one-photon photoemission (1PPE) near the threshold using visible and ultraviolet laser light.[4,8] Measurements on a perpendicularly magnetized Co film on Pt(111) also demonstrate a remarkable asymmetry of 11.7% directly at threshold in two-photon photoemission (2PPE) using ultrashort pulsed laser light.[10] Both results indicate MCD in near-threshold photoemission as a potential candidate for time-resolved magnetic imaging using photoemission electron microscopy[11] and thus might pave the way for a future MCD-based investigation of ultrafast magnetization dynamics.[12]

However, single- and multiphoton photoemission processes near the threshold are not only interesting with respect to future applications but also from the viewpoint of fundamental research.[13–15,25] For instance, the conventional photoemission model successfully describes most photoexcitation processes (particularly in the regime of $h\nu > 10$ eV) by direct band-to-band transitions with $k_{||}$ conservation. This is particularly true for photoemission along the direction of normal electron emission. Nevertheless, it cannot be applied in every case. This was, for example, shown by photoemission experiments on Ag(111) where an *extra* intensity occurs on the low binding energy shoulder of a direct interband transition peak and which was attributed to indirect transitions induced by the surface.[16] The so-called "surface photoemission" originates from the $\vec{\nabla} \cdot \vec{A}$ term in the perturbation operator.[17,18] In addition, our MCD measurements on Co(111) cannot be explained in the framework of conventional photoemission theory since excitations in the direction of normal electron emission (Γ-L) can only lead to evanescent final states for 1PPE as well as for 2PPE at the corresponding photon energies.[10] Previous thickness-dependent MCD measurements, however, clearly revealed that excitations into final evanescent states must be excluded.[9] Instead, the MCD asymmetry is traced back to direct interband transitions in k directions deviating from the Γ-L direction. As a consequence, additional momentum has to be transferred to the electron to surmount the surface barrier after the photoexcitation process. This is assumed to be provided by electron-phonon and/or electron-magnon scattering processes.[10]

Calculations on the basis of this model have been performed, averaging over all allowed band-to-band transitions (i.e., those fulfilling the relativistic dipole selection rules) in all k directions of the Brillouin zone and additionally taking into account the Einstein equation of photoemission [i. e., considering only those transitions for which $h\nu > \Phi$ ($2h\nu > \Phi$) for 1PPE (2PPE); Φ, work function]. For 1PPE the predicted MCD asymmetries are in reasonable

agreement with the experiment.[10] Note, that the calculations for this nonconventional approach are in strong analogy to calculations for the magneto-optical Kerr effect (MOKE). However, beyond the MOKE ansatz, an additional requirement of energy conservation in the photoemission process is implemented. For the 2PPE case only the first excitation step could be treated theoretically due to the lack of a real final state. It turned out that the asymmetry is related to a few specific transitions in the first excitation step. Nothing is known on the role of the intermediate state and the influence of the second excitation step with respect to the circular dichroism.[10] Especially, the question remains whether both excitation steps contribute equally to the asymmetry or whether one of the steps is the major asymmetry-generating process.

To gain further insight into these open questions we first studied a 2PPE transition at $h\nu = 2.92$ eV and high work function $\Phi = 4.98$ eV .[10] Here we lower the work function to about $\Phi = 2.2$ eV, so that the corresponding 1PPE channel for a photon energy of $h\nu = 3.06$ eV (which is close to $h\nu = 2.92$ eV) opens. This means that the second excitation step of the 2PPE transition is "switched off" and we obtain a 1PPE process which might be equivalent to the first excitation step of the 2PPE process. This enables the comparison between the MCD of a one-step process and the MCD of the corresponding two-step process so that we gain immediate information about the MCD contribution inherent in the first excitation step. The 1PPE measurement is finally compared to *ab initio* calculations of the 1PPE asymmetry.

Moreover, the calculations as well as the experiments presented in Ref. 10 point out that the existence of a real intermediate state might be important for obtaining large 2PPE-MCD asymmetries. In order to prove this idea, the 2PPE photon energy is adjusted in a way that excitations into real intermediate states are triggered at low work-function values. This enables measurements of the 2PPE MCD asymmetries which originate from different interband transitions than discussed in Ref. 10 and therefore reveals the influence of a real intermediate state independent of the energy range probed in the band-structure scheme. Energy-dependent 2PPE measurements are carried out in the range of $h\nu = 1.53$–1.66 eV [i.e., at the same total transition energy as used in the 1PPE case ($h\nu = 3.06$ eV)].

II. EXPERIMENTAL

A Co film of 4.5 monolayers (ML) thickness is grown on a Pt(111) substrate. Before deposition the Pt(111) single crystal is cleaned by Ar-ion sputtering (120 min, $p \sim 4 \times 10^{-6}$ mbar) and subsequent annealing (30 min, 670 °C) at a pressure of $p \sim 4 \times 10^{-9}$ mbar. In the regime of a few monolayers Co/Pt(111) the easy magnetization axis is oriented along the surface normal ,[19–21] which is promising for large MCD signals. The investigation of 4.5 ML of Co furthermore facilitates the analysis of the results in terms of an fcc Co bulk band structure. The deposition is carried out at room temperature and 5×10^{-10} mbar by electron beam evaporation at a rate of 1 ML/4.5 min. The epitaxial growth of the film is controlled by low energy electron diffraction (LEED) while the magnetic properties are determined by *in situ* measurements

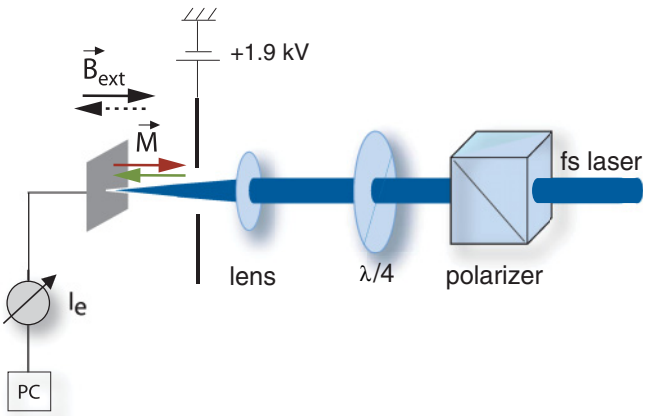

FIG. 1. (Color online) Schematic drawing of the experimental setup for MCD measurements near the photoemission threshold in the polar setup. Photon energy is $h\nu = 3.06$ eV for 1PPE and $h\nu = (1.53$–$1.66)$ eV for 2PPE.

of the polar magneto-optical Kerr effect (PMOKE). After LEED and MOKE characterization the MCD measurements are carried out. Figure 1 depicts a schematic drawing of the experimental setup: For 1PPE continuous wave (cw) laser light with an energy of $h\nu = 3.06$ eV (405 nm, 1.5 mW) is used. For 2PPE we use the first harmonic of a broadband ultrashort pulse laser (<100 fs, 80 MHz repetition rate) with photon energies ranging from $h\nu = 1.53$–1.66 eV. To generate 2PPE processes an additional lens ($f = 15$ mm) is mounted in the vacuum chamber with its focal point at the sample surface. Possible admixture of higher harmonics is cut off by an optical filter. By means of an aperture and a lens the particular laser beam is adjusted into the vacuum chamber, where the sample is placed between the pole shoes of an electromagnet generating a magnetic field of up to ±1000 Oe for 1PPE (±1500 Oe for 2PPE) at the sample position during MCD measurements. Circular polarization is produced by a combination of a linear polarizer and a quarter wave plate for the particular wavelength. The photoemitted electrons are measured by the drain current from the sample upon placing an anode plate (1900 V) in front of the sample. During all measurements the magnetization vector is oriented along the surface normal and parallel or antiparallel to the helicity vector of the incoming laser light. All measurements are carried out at room temperature.

III. RESULTS

After sample preparation and LEED polar Kerr measurements are carried out under 45° incidence of 636-nm laser light revealing an easy axis magnetization curve. This confirms that the magnetization is oriented along the surface normal.

In order to decrease the work function from ∼5.0 eV for clean Co/Pt(111), Cs is deposited onto the sample surface. Figure 2 shows the dependence of the sample current at $h\nu = 3.06$ eV on the Cs exposure time. After 25 min the work function has decreased to the threshold value of 3.06 eV and emission sets in. The current signal increases and reaches a maximum value after 48 min of Cs dosage.

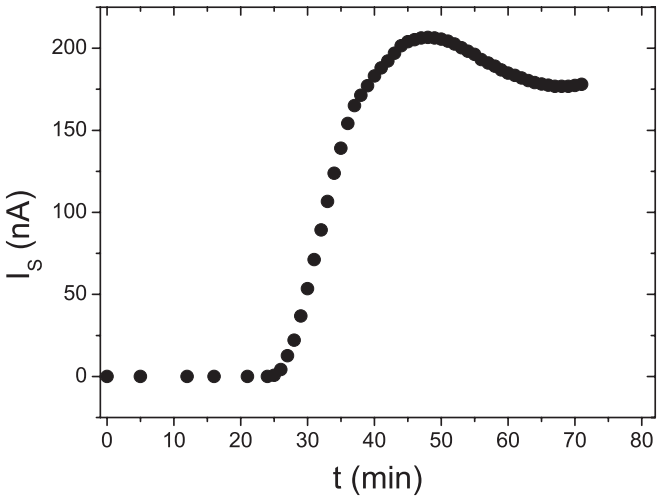

FIG. 2. Dependence of sample current on the duration of Cs dosage for a 4.5-ML Co film on Pt(111) measured at $h\nu = 3.06$ eV.

This maximum corresponds to a work function minimum of 1.63 eV at 0.65 ML cesium coverage. These values were found for Cs/W(110),[22] and in the following we assume that with respect to the sample work function both systems Cs/W(110) and Cs/Co/Pt(111) behave similar. Further dosage leads to a rise of work function visible in the drop of sample current. Referring to Ref. 22 a fully cesiated W(110) sample yields a work function in saturation of ∼2.11 eV. After 71 min the sample is saturated and the Cs dosage is stopped. Before MCD measurements are carried out the approximate value of the work function is checked by measuring the sample current with a photon energy of 1.95 eV. No current signal is measured which means that the work function is larger than 1.95 eV, in agreement with Ref. 22.

A. 1PPE measurements

The 2PPE transition at a photon energy of $h\nu = 2.92$ eV and a sample work function $\Phi_{2PPE} = 4.98$ eV studied in Ref. 10 yielded an asymmetry value of 8.37 %. Here we map the first excitation step as a real 1PPE process. To this end, the sample work function is reduced to a value of $\Phi \sim 2.2$ eV by means of Cs adsorption, and an appropriate photon energy of $h\nu = 3.06$ eV (which is close to the value of 2.92 eV) is used. Figures 3(a) and 3(b) show the energy schemes of the 2PPE and 1PPE transitions.

Figure 4 depicts the 1PPE MCD measurement directly after cesium adsorption. The data points represent the average of 30 hysteresis loops; each loop consists of 160 current readings. The square loops prove that the magnetization easy axis points along the external field normal to the sample plane. The MCD asymmetry is evaluated as

$$A_{\mathrm{MCD}} = \frac{\overline{I_S}^{M^+} - \overline{I_S}^{M^-}}{\overline{I_S}^{M^+} + \overline{I_S}^{M^-}},$$

where $\overline{I_S}^{M^+}$ ($\overline{I_S}^{M^-}$) are the averaged values of the sample currents for positive (negative) sample magnetization direction measured for fixed photon helicity. This evaluation procedure is also used for the 2PPE case. The measurement in Fig. 4 yields an asymmetry of 5.89 %.

With increasing time after stopping of the Cs deposition the work function starts to increase from the saturation value of 2.11 eV due to contamination by residual gas adsorption. A time-dependent measurement thus enables detecting the 1PPE MCD asymmetry at varying work function values and especially at $\Phi = 2.2$ eV needed for comparison with the former 2PPE experiment. Furthermore, the general dependence of the asymmetry on a varying sample work function can be investigated. Within 320 min 626 asymmetry values are recorded. For each asymmetry value one hysteresis

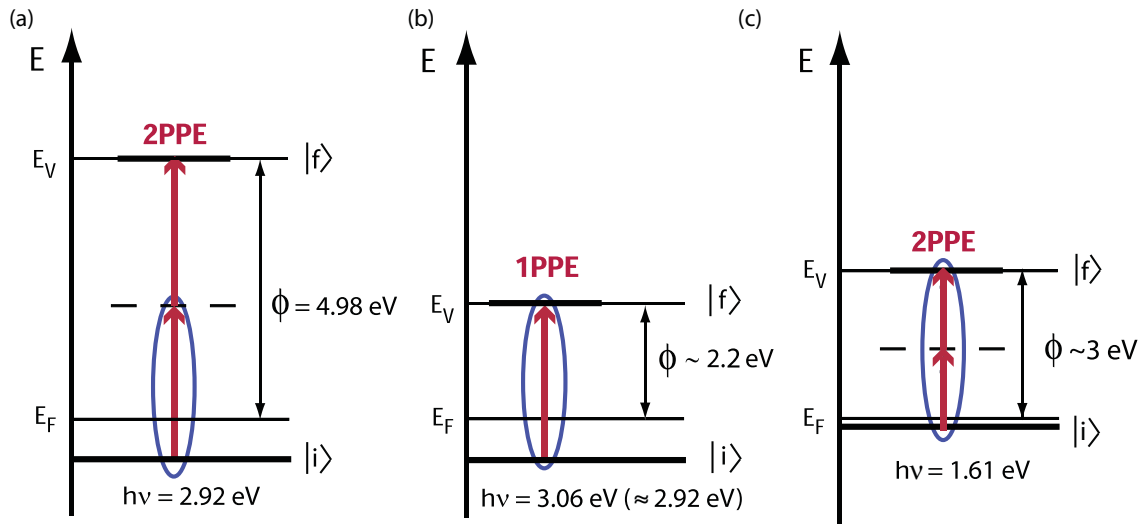

FIG. 3. (Color online) Energy schemes for the 2PPE process at $h\nu = 2.92$ eV (a), the 1PPE process at approximately the same photon energy (b), and the 2PPE process at $h\nu = 1.61$ eV (c). E_F and E_V denote the Fermi energy and the vacuum level, $|i\rangle$ and $|f\rangle$ the initial and final states of the phototransition, respectively; for the sketch $|f\rangle$ is assumed to be positioned at the vacuum level (i.e., excitation of electrons with maximum binding energy). In order to obtain 1PPE transitions the work function is reduced by Cs adsorption from approximately 5 eV (a) to ∼2.2 eV (b) and ∼3 eV (c).

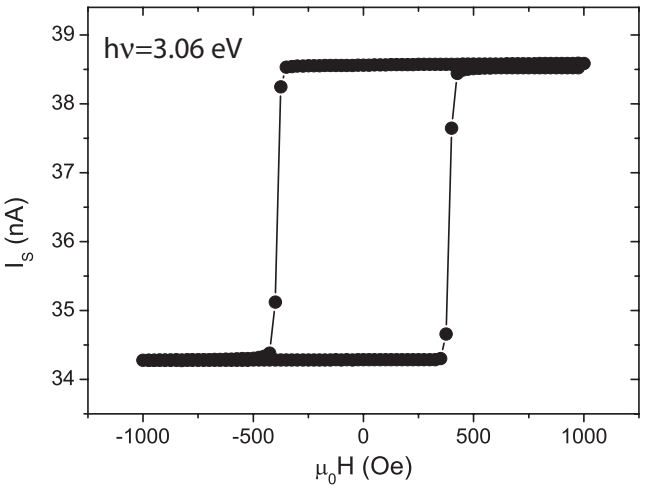

FIG. 4. 1PPE MCD measurement showing the sample current at a photon energy of $h\nu = 3.06$ eV. The figure represents an average over 30 hysteresis loops; the error bars are in the order of the symbol size.

loop is acquired and the asymmetry is calculated by using the current values in remanence. In order to display the dependence of the asymmetry on the excess energy $h\nu$-Φ, the measurement time is translated to work function values. For this conversion the dependence of the average sample current on the work function is derived from the initial Cs deposition experiment shown in Fig. 2 assuming a linear relation between coverage and deposition time and using the relation between coverage and work function known from Ref. 22. Figure 5 shows the dependence of sample current and asymmetry on the excess energy $h\nu$-Φ. The sample current (a) increases continuously for both magnetization directions with decreasing work function. The asymmetry curve (b) shows a linear increase at low work functions (right side) until a shallow maximum of 6.21% is reached at $h\nu$-$\Phi = 0.61$ eV. Here the slope changes sign and the asymmetry decreases linearly to a value of 4.4% at threshold (dashed line). The initial increase in asymmetry to the maximum is associated with particular electronic excitations. This will be discussed in detail below. At a work function of $\Phi = 2.2$ eV an asymmetry of 6.00% is reached. This enables a direct comparison to the mentioned 2PPE case and will be discussed later as well. Asymmetries below threshold, where $h\nu$ is smaller than Φ (left-hand side of dashed line) were already reported in Ref. 10 and are attributed to finite temperature and photon energy broadening effects. Furthermore, an excitation of electrons below the macroscopic work-function threshold due to local inhomogeneities of the surface cannot be excluded since the work function of such defects is locally reduced.[30] The increased statistical scatter in the asymmetry values below threshold is attributed to small sample currents in the low nA range in the subthreshold region.

B. 2PPE measurements

For the 2PPE experiments Cs is dosed on a freshly deposited Co film. After Cs deposition no current signal is detected for photon energies lower than $h\nu = 1.95$ eV. Using pulsed laser light and a focusing lens in close distance to the sample the

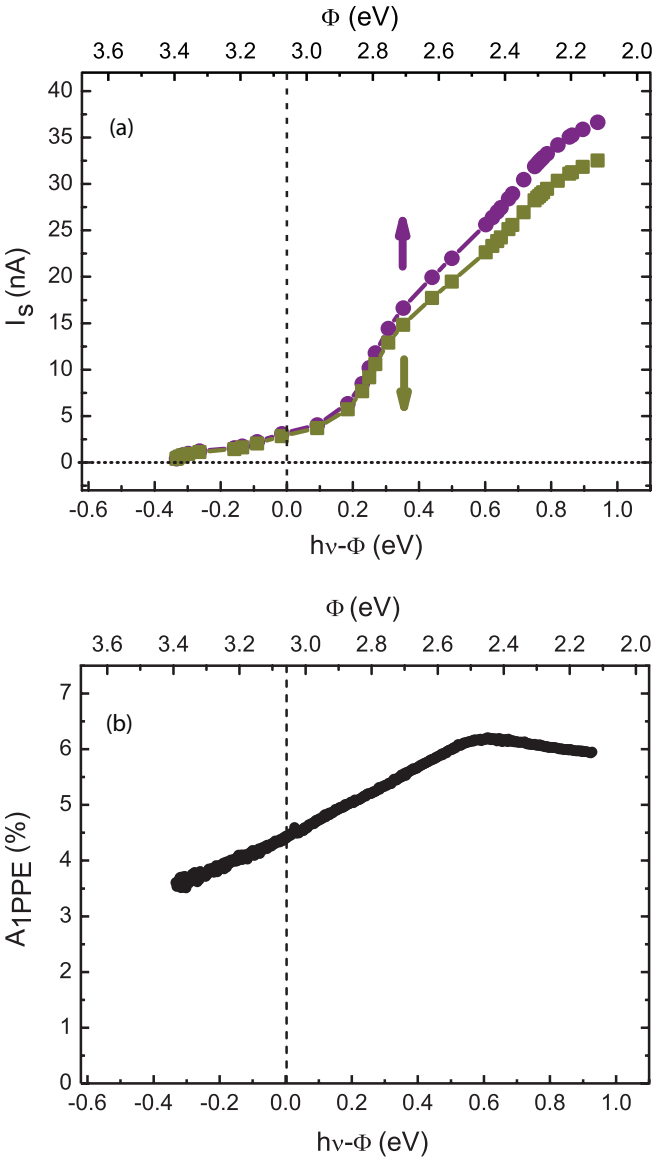

FIG. 5. (Color online) (a) Dependence of the sample current on the excess energy $h\nu$-Φ at $h\nu = 3.06$ eV for both magnetization directions. (b) Corresponding asymmetry curve. The dashed line denotes the photoemission threshold.

photon intensity is increased allowing for 2PPE processes. Now, a sample current appears for a 2PPE energy exceeding $2h\nu = 3.06$ eV. The work-function value can therefore be estimated to be $\Phi \approx 3$ eV. To trigger excitations to real intermediate states different from those excited in the 2PPE measurement of Ref. 10 we choose a photon energy of $h\nu = 1.61$ eV. This yields $A_{2PPE} = 16.8\%$. Figure 3(c) depicts a sketch of the 2PPE process; Fig. 6(a) shows the corresponding 2PPE measurement for which 30 hysteresis loops are averaged. Each hysteresis loop consists of 240 current readings. In Fig. 6(b) the spectral variation of the 2PPE asymmetry is plotted in the energy range of $2h\nu = 3.06$–3.31 eV. Unlike the 1PPE case, we find an almost constant asymmetry independent of the photon energy. An average value of about 17% persists in the full photon energy range investigated.

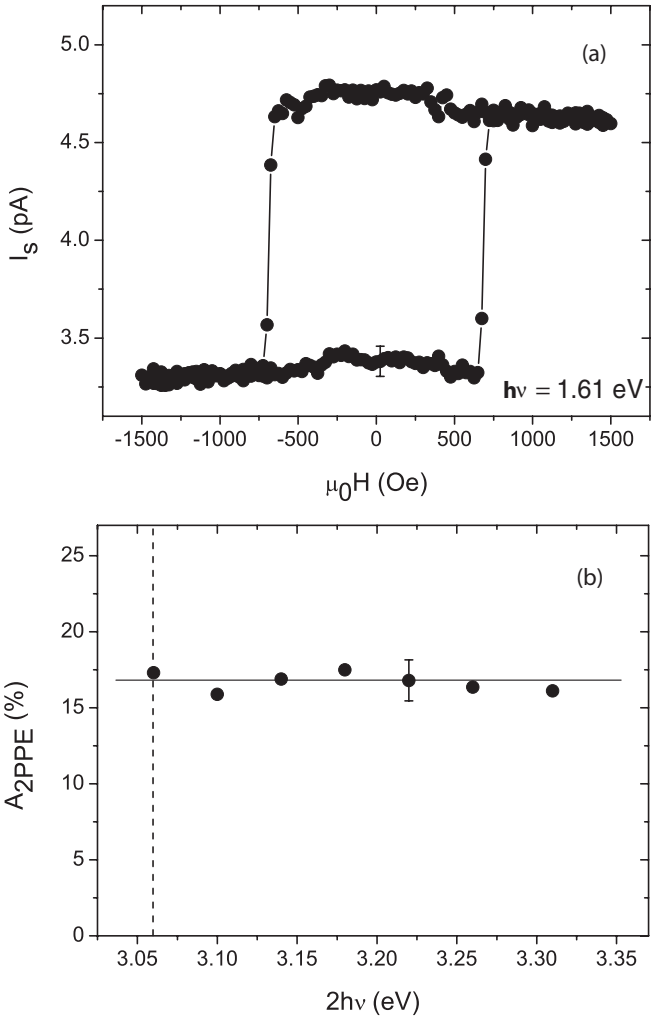

FIG. 6. (a) 2PPE MCD measurement at hν = 1.61 eV. A typical error bar that is mainly due to the detection of small sample currents is shown on the bottom branch. (b) Photon-energy dependence of the 2PPE MCD asymmetry. A characteristic error has been derived exemplarily for 3.22 eV. The dashed line denotes the photoemission threshold (with an error of ±0.1 eV).

IV. DISCUSSION

As a prior condition for the following discussion the Cs adsorption (and residual gas adsorption) is assumed to have a negligible influence on the bulk electronic structure and the bulk magnetic properties of the Co/Pt sample systems. This is justified by two reasons. First, an influence of alkali and even oxygen adsorption is only restricted to the surface region of materials.[23,24,27,29] The bulk properties remain unaffected.[25] Several studies reveal that in the surface region the electronic structure and the magnetic properties of only the topmost surface layer are affected by the deposition.[26–29] Second, it was shown that magnetic circular dichroism for Co films on Pt is a bulk-sensitive effect.[9] Similar results have been gained for Ni(001).[4] This means that the influence of the surface, even when it was heavily modified by Cs deposition, does not play a significant role. A missing influence of Cs on the magnetic properties of the sample system is moreover directly demonstrated by the present study. Upon Cs adsorption the Kerr signal from the Co film does not change. This is a clear indication that both the magnetization and the magnetic anisotropy of the system remain unaffected; there is no detectable influence on the surface and bulk magnetic properties. This also points out that the bulk electronic structure might not be changed in the case of Cs/Co/Pt(111).

A. 1PPE measurement

Unlike almost all cases studied so far, the MCD asymmetry of Cs/Co/Pt(111) increases with increasing excess energy in 1PPE [Fig. 5(b)]. A prominent counterexample is Cs/Ni/Cu(001) where the asymmetry drops to zero within the first 600 meV above threshold. The 1PPE asymmetry curve in Fig. 5(b), however, still reveals an asymmetry value of 5.95% at an excess energy of 0.93 eV (implying a binding energy interval from 0 to 0.93 eV). This proves that the MCD asymmetry in the case of Co(111) is not threshold sensitive, in striking contrast to the Ni(100) case.

The results shown in Fig. 5 enable a direct comparison with the 2PPE measurement of Ref. 10. While for 2PPE an asymmetry of 8.37% (hν = 2.92 eV, Φ = 4.98 eV) has been detected, the 1PPE measurement already yields a value of 6.00% (hν = 3.06 eV, Φ = 2.2 eV). This comparison reveals that the first excitation step delivers already 72% of the 2PPE asymmetry. This leads to the conclusion that the first excitation step is the dominant asymmetry-generating process in this case.

To explicitly interpret the origin and the behavior of the 1PPE asymmetry in dependence of the excess energy it is worth analyzing possible excitation pathways within a spin-resolved band structure calculation for Co. Figure 7 shows a fully relativistic calculation for the low index crystallographic directions of fcc Co on the basis of spin density functional theory and local spin density approximation using a lattice constant of $a = 3.5457 \times 10^{-10}$ m. The bands are labeled by numbers starting from the lowest valence band. The length of bars at each line marks the strength of the d character of the particular bands ("fat band representation"). Vertical arrows denote possible transitions for 1PPE (dashed) and 2PPE (full arrows). Note that for reasons of clarity only the high symmetry directions are shown. In the full three-dimensional (3D) k space many more transitions in arbitrary k directions are possible. For 1PPE the accessible regime of final-state energies is marked as shaded area. For 2PPE the estimated work-function value (∼3 eV) is marked by a dashed line. Following the model for near-threshold photoemission discussed in Ref. 10, we will look in particular for direct interband transitions in directions deviating from Γ-L, where real intermediate states in 2PPE or real final states in 1PPE are involved. The conventional model of photoemission only allows for direct transitions ($\Delta k_{||} = 0$). For near-threshold photoemission we have in addition $k_{||} \approx 0$ [i. e., photoemission in the direction along Γ-L of the Brillouin zone from a (111) surface]. In the case of Co(111) these transitions can only proceed through virtual intermediate states (for 2PPE) and final evanescent states at the corresponding photon energies in the near-threshold region. However, bulk sensitivity, that is, the increase of the MCD asymmetry up to large thicknesses

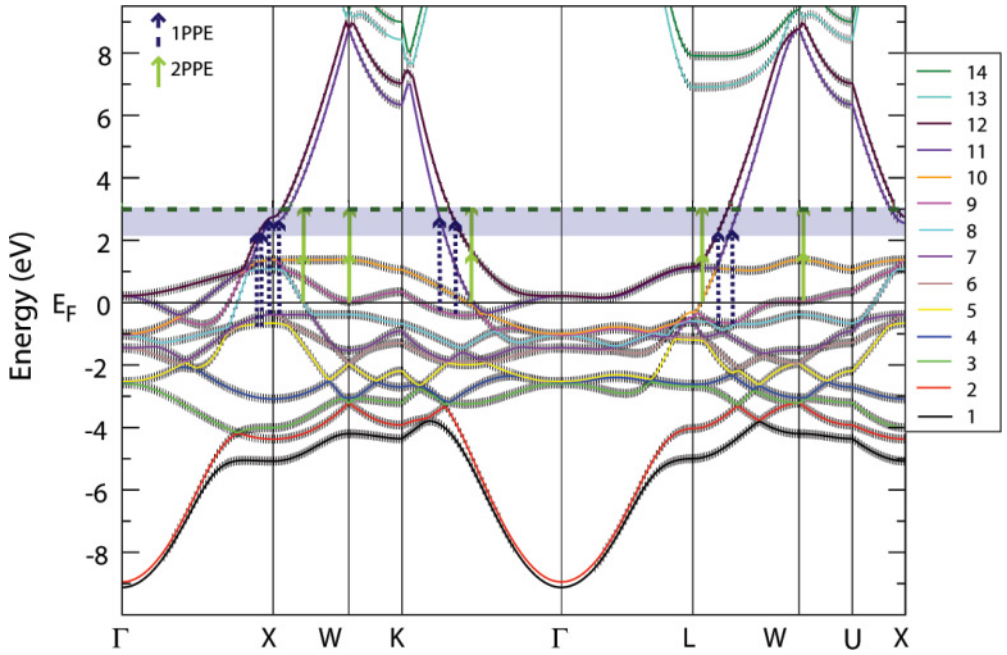

FIG. 7. (Color online) Relativistic band structure calculation for fcc Co (lattice constant $a = 0.35457$ nm). For each band the d character is indicated by small bars (i. e., the length of the bars reflects the amount of pure d character of the corresponding band). The dashed (continuous) arrows show possible 1PPE (2PPE) transitions. The shaded area denotes the range in which the work function has been varied ($\Phi = 2.13$–3.06 eV) during the 1PPE measurement. The dashed line at 3 eV marks the estimated value of the vacuum level E_V for the 2PPE measurement.

of eight monolayers was reported for a Pt/Co/Pt trilayer.[9] This result demonstrates that the relevant final state (or the intermediate state in the 2PPE process) must stem from the bulk band structure. Excitations to evanescent final states (or evanescent intermediate states in the 2PPE process) must therefore be excluded. It is thus near at hand to consider directions different from Γ-L, where interband transitions into real intermediate and real final state bands are possible. At $\Phi = 2.45$ eV (maximum binding energy 0.61 eV) the 1PPE asymmetry shows a maximum value of 6.2%, indicating that particular transitions might show a strong relative contribution at that work-function value. This can also be recognized by analyzing the increase in asymmetry from 4.4% at threshold to 6.2% at $h\nu$-$\Phi = 0.61$ eV. Increasing the binding energy from 0 to 0.61 eV implies the onset of several band-to-band transitions in the crystallographic directions Γ-X and Γ-K. In all possible transitions bands 11 and 12 serve as final states. While in Γ-K only band 9 serves as initial state, bands 6 and 7 are the appropriate initial states in the Γ-X direction. Here, all excitations take place in the vicinity of the high-symmetry X point, where the initial as well as the final states carry a high density of states leading to high transition probabilities. Furthermore, the band-structure scheme indicates that the final bands 11 and 12 exhibit pure p character directly at X while the initial states are d states. This means that due to the dipole selection rules the highest transition strengths arise in the vicinity of the X point. At work-function values <2.45 eV, further contributions from the initial bands 5 in Γ-X and 8 and 9 in L-W set in. These onsets might be a reason for the slight reduction of the 1PPE asymmetry to 5.95% at a maximum binding energy of 0.93 eV.

Figure 8(a) shows a spin-resolved calculation of the imaginary and real parts of the conductivities σ_{xy} and σ_{xx} for the 1PPE excitation as a function of photon energy, using a computational scheme adapted from Ref. 31 to include the work function. The green curve gives the conductivity spectra due to majority-spin excitations, the red curve those due to minority-spin transitions. A work function of 2.0 eV and a typical lifetime broadening of 0.4 eV of the final state are assumed. The figure approximately reflects the situation at the end of the experimentally probed range with a highest excess energy of $h\nu$-$\Phi = 0.93$ eV in Fig. 5(b). At a photon energy of $h\nu = 3.06$ eV the MCD-related terms $\mathrm{Im}[\sigma_{xy}]$ and $\mathrm{Re}[\sigma_{xx}]$ already yield an average asymmetry value of $A_{1\mathrm{PPE}} \sim 1.5\%$ using the crude approximation $A_{1\mathrm{PPE}} = \frac{\mathrm{Im}[\sigma_{xy}]}{\mathrm{Re}[\sigma_{xx}]}$ and considering all possible transitions. In analogy to the 1PPE calculations of Ref. 10 yielding an average asymmetry of ∼2.5% for $h\nu = 3.06$ eV and $\Phi = 2.49$ eV, the value of 1.5% for $h\nu = 3.06$ eV and $\Phi = 2$ eV is smaller than the experimentally detected asymmetry of ∼5.95% at $h\nu = 3.06$ eV and $\Phi = 2.13$ eV. The trend of increasing asymmetry with increasing work function fits the experimental observation [Fig. 5(b), to the right of the maximum]. A possible reason for the remaining difference between experiment and theory might not only be the fact that Fig. 5 is accompanied by several approximations concerning the determination of work-function values. Another reason might also be attributed to a selection mechanism in the phonon-scattering process. In theory all k directions are averaged equally. In reality phonon scattering with lower momentum transfer is more probable than scattering with higher momentum transfer. This would favor k vectors with larger projection onto the surface normal

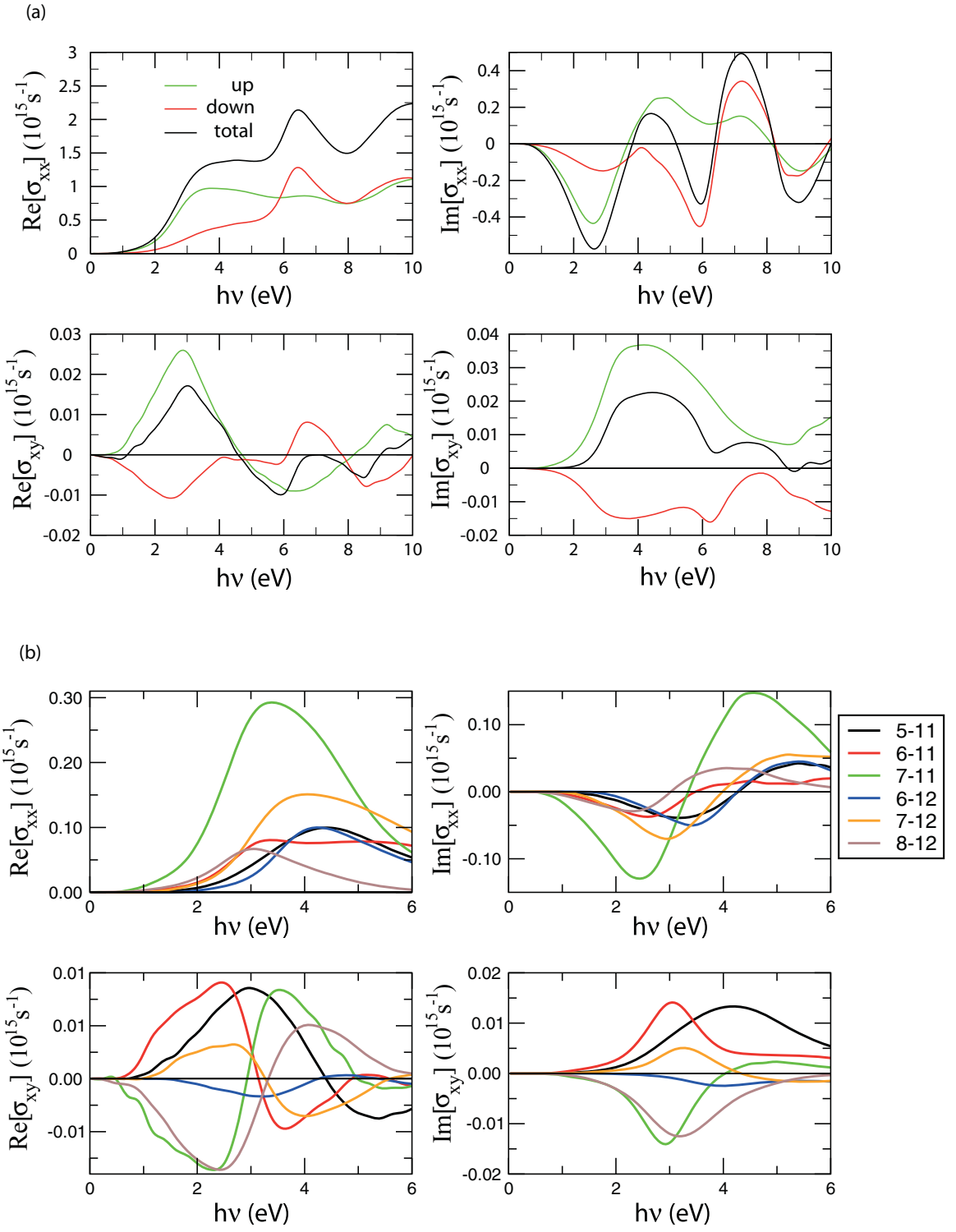

FIG. 8. (Color online) (a) Calculated spin-resolved 1PPE optical conductivity spectra. The imaginary and real parts of σ_{xx} and σ_{xy} for 1PPE are shown as a function of the photon energy. (b) Calculated band-resolved conductivity spectra. A work function of 2.0 eV and a lifetime broadening of 0.4 eV are assumed. The colors code the band transitions according to band numbers given in Fig. 7.

against those with a smaller one. Moreover, the fact that the experimental as well as the calculated 1PPE asymmetries are smaller than those measured for 2PPE points out that for Co(111) enlarged asymmetries are only reached with two excitation steps passing an intermediate state.

Further insight is given by Fig. 8(b) which depicts a band-resolved calculation of the conductivities for 1PPE. Calculated are the real and imaginary parts of σ_{xy} and σ_{xx} for the most relevant interband transitions. Especially the transitions from bands 6, 7, and 8 to bands 11 and 12 contribute

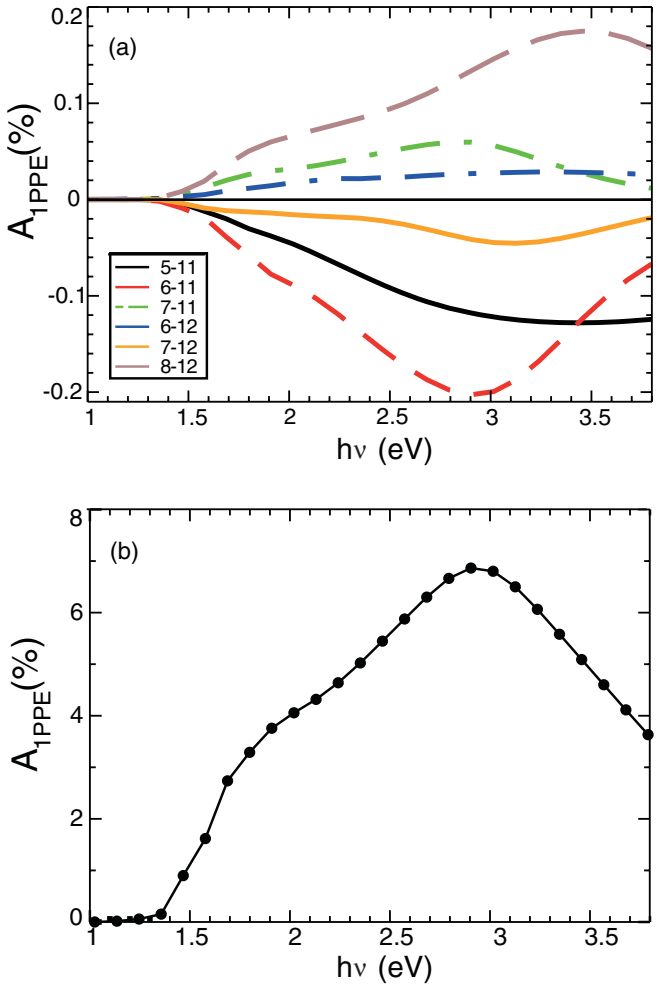

FIG. 9. (Color online) (a) Calculated 1PPE MCD asymmetry in dependence of the photon energy for the most relevant interband transitions. (b) Averaged asymmetry versus photon energy arising from the two dominating transitions $7 \rightarrow 11$ and $8 \rightarrow 12$. A work function of 2.0 eV and a lifetime broadening of 0.27 eV are assumed.

with enlarged single transition asymmetries. Calculating the asymmetry at $h\nu = 3.06$ eV transitions $7 \rightarrow 11$, $7 \rightarrow 12$, and $6 \rightarrow 12$ reveal absolute asymmetries between 3% and 5%. Much larger absolute asymmetries of about 15% and 19% are connected with the transitions $8 \rightarrow 12$ and $6 \rightarrow 11$. However, the contribution from the $6 \rightarrow 11$ interband transition is heavily reduced when averaging over all participating transitions as already mentioned in Ref. 10. In contrast, in Ref. 10 transition $7 \rightarrow 11$ was supposed to be the most asymmetry-dominating interband transition, because it dominates the optical intensity in the vicinity of the work function. In fact, with an asymmetry value of ~4.6% it almost reproduces the result of our 1PPE measurement (5.95% at $\Phi = 2.13$ eV).

These results are summarized in Fig. 9(a) where the 1PPE MCD asymmetry is plotted in dependence of the photon energy for single band-to-band transitions.

All possible interband transitions with considerable contributions to the asymmetry are shown for a work function of 2.0 eV and a lifetime broadening of 0.27 eV. In Fig. 9(b) we have additionally plotted the average asymmetry versus photon energy for the 1PPE process. For the calculation of the asymmetry only the two transitions $7 \rightarrow 11$ and $8 \rightarrow 12$ are chosen since in the vicinity of the threshold they contribute most. At $h\nu = 3.06$ eV the average asymmetry value yields 6.6% which is in good agreement with the experimental value of 5.95%. The calculation nicely demonstrates that for the case of Co(111) specific single interband transitions govern the MCD asymmetry in near-threshold photoemission. They are enhanced with respect to others by a selection mechanism like phonon scattering in the bulk or at the surface. Obviously, the contribution from $8 \rightarrow 12$ leads to a further increase in asymmetry. However, at $h\nu = \Phi = 2$ eV and up to 0.5 eV above threshold the main contribution arises from the $7 \rightarrow 11$ transition as can also be seen in the plot of σ_{xx} in Fig. 8(b). Calculations performed using a very small broadening (not shown here) reveal that the contribution of other transitions (mainly $6 \rightarrow 11$, $5 \rightarrow 11$, and $7 \rightarrow 12$) starts to set in at $h\nu - \Phi \geqslant 0.5$ eV. If these further contributions from other interband transitions are taken into account, in combination with a lifetime broadening of 0.4 eV, the resulting MCD asymmetry is reduced. This is also reflected by the discussed value of 1.5% as the first approximation of the averaged asymmetry arising from all possible interband transitions. This is a strong argument for the concept of a selection mechanism.

Note that for the above discussion lifetime broadening has been taken into account since all excited real electronic states (final and intermediate states) are lifetime broadened and cannot be regarded as sharp lines. The importance of lifetime broadening becomes evident checking the origin of the 1PPE asymmetry directly at threshold: As shown in the band-structure scheme no band crosses the Fermi level in regions where an excitation to a real final state is possible. Only by including a typical lifetime broadening of 0.2–0.4 eV excitations become feasible.

B. 2PPE measurement

To gain more information about the role of real intermediate states in a two-step process, 2PPE measurements are carried out for a different photon energy range ($h\nu = 1.53$–1.66 eV) as compared to Ref. 10. The measurement [Fig. 6(b)] yields an almost constant asymmetry of 17%, which is larger than the 2PPE asymmetry (8%–12%) in the photon energy range $h\nu = 2.46$–2.92 eV [Fig. 5(b) of Ref. 10]. Assuming 3 eV as the lowest limit for the work-function value, electrons can stem from initial bands with a maximum binding energy of 0.31 eV. In analogy to the 1PPE measurement the enlarged asymmetry values might be explained by direct transitions along crystallographic directions other than Γ-L. Here, photon energies in the range of 1.53–1.66 eV are expected to connect initial states with real intermediate states. Referring to the band-structure scheme the final states of these two-step processes are evanescent. This is comparable to the 2PPE measurement in Ref. 10. However, since the used photon energies are different, other transitions are excited resulting in different asymmetry values.

Electrons from close to the Fermi level can be excited in four low-index crystallographic directions, X-W, Γ-K, L-W, and W-U as shown in Fig. 7. Besides the transition $8 \rightarrow 10$ in

the X-W direction, the transition $9 \rightarrow 10$ might be of particular interest since it takes place directly at the W point, and initial as well as intermediate states carry a high density of states associated with large transition probabilities. However, one should keep in mind that in addition to the energy conservation the dipole selection rules have to be obeyed. In this context, the excitation from band 9 to band 10 might be suppressed or at least strongly reduced since both bands carry strong d character directly at the W point (Fig. 7).

In the Γ-K direction bands 10 and 11 are the possible initial and band 12 a suitable real intermediate state in the middle of the Γ-K scale. Additionally, a transition from band 10 to 12 exists in the L-W direction. Since it takes place in the vicinity of L where band 10 exhibits p character and band 12 carries d character, this transition is also a candidate for high MCD asymmetries. Furthermore, the vicinity to the high-symmetry point L favors the excitation and could even enable a direct transition in the normal emission direction Γ-L without participation of any scattering processes. All mentioned transitions directly set in at the threshold $h\nu \approx \Phi$ and still contribute at higher photon energies due to lifetime broadening. This is also reflected by the constant 2PPE MCD asymmetry.

In summary, the present 2PPE measurement proves that excitations into real intermediate states lead to large 2PPE asymmetries independent of the probed energy region in the band-structure scheme. Further statements concerning the influence of the second excitation step are not possible as long as evanescent states are involved which cannot be described by our theoretical approach. This inhibits a direct comparison between experiment and theory for a complete 2PPE transition.

Finally it is worth mentioning that MCD measurements under variation of the photon energy do not directly correspond to experiments under variation of the sample work function. In both approaches a particular asymmetry is reached directly at threshold. With increase of photon energy the length of the "arrows" connecting initial and final states in the transition scheme becomes larger while the vacuum level stays fixed. Therefore, the possible asymmetry-generating transitions differ from each other, so that the variation of MCD asymmetry vs photon energy arises from the *energy selectivity* of the electronic excitations. Of course, lifetime broadening smears out the spectral variations. For experiments under variation of the work function the situation is different. Lowering the work function from the threshold value ($\Phi = h\nu$) at a fixed photon energy leads to an opening of more and more electronic excitation channels (interband transitions). This is also the reason for the increase of the 1PPE asymmetry from $\Phi = 3.06$ eV to its maximum at $\Phi = 2.45$ eV in Fig. 5(b). Here, the existence of lifetime broadening weakens the instantaneous onset of new channels. In this context the theoretical calculations for two Heusler systems also demonstrated that a variation of photon energy compared to a variation of work function leads to different MCD values.[7]

V. CONCLUSION

Magnetic circular dichroism in one- and two-photon photoemission (1PPE and 2PPE) near the threshold has been investigated for Cs/4.5 ML fcc Co/Pt(111) sample under wide-range variation of the sample work function in the case of 1PPE and variation of the photon energy at low work function for 2PPE. In the 1PPE case ($h\nu = 3.06$ eV) the asymmetry values reveal a nonmonotonous behavior in dependence of the excess energy $h\nu$-Φ. Unlike the Cs/Ni/Cu(100) case [4] the asymmetry increases with increasing excess energy from its threshold value of 4.4% to a kinklike maximum of 6.2% at $h\nu$-$\Phi = 0.61$ eV, followed by a shallow drop to 5.95%. The 1PPE result is traced back to direct interband transitions in k directions other than the direction of observation (Γ-L) following a model introduced in Ref. 10. The 1PPE result shines new light on the influence of the first excitation step in a 2PPE process. Since it maps the first excitation step of a previously studied 2PPE measurement,[10] we can conclude that the first step gives the major contribution to the total MCD. The transition from the intermediate state to a final evanescent state in the 2PPE transition (assuming sequential excitation) further increases the asymmetry from 6.0% to 8.3%. *Ab initio* calculations of the 1PPE MCD are performed adopting the model from Ref. 10 usually used for the magneto-optical Kerr effect (MOKE) with additional restriction in energy due to the existence of the sample work function in the photoemission process. The theory yields an averaged asymmetry value for the two dominating transitions that is in good agreement with the measured asymmetry. This is a strong argument for the concept of a selection of particular interband transitions by phonon scattering causing enhanced MCD asymmetries.

Larger asymmetry values only seem to be reachable by means of a real intermediate state and a second excitation step. To sustain this assumption 2PPE measurements in a different photon energy range ($h\nu = 1.53$-1.66 eV) are compared to previous experiments in Ref. 10. Energy-dependent measurements at decreased work function yield almost constant asymmetries with maximum values of about 17%. The enlarged asymmetry values can again be explained by direct interband transitions in crystallographic directions other than Γ-L. Since this measurement also yields an enhanced 2PPE asymmetry, one can conclude that at least for the case of Co(111) the involvement of a real intermediate state and a second excitation step cause an enhancement of the asymmetry independent on the probed energy range. The origin of the enhancement of the 2PPE signal with respect to the 1PPE case can also be related to different selection rules for 1PPE and 2PPE. While for 1PPE the parity is changed in the excitation process it does not change in the case of 2PPE. Principal differences between 1, 2, and 3PPE processes also show up in spin-resolved measurements as discussed by Winkelmann *et al.*[13,25] Additionally we notice that the asymmetry increases by decreasing the available binding energy range. This observation cannot be generalized since only two measurements have been carried out so far, and the enhanced asymmetry values could also be associated with particular band-structure features.

ACKNOWLEDGMENTS

This work was supported by the Carl-Zeiss-Stiftung and the MAINZ Graduate School of Excellence (Kerstin Hild), the

Deutsche Forschungsgemeinschaft (Grant No. EL 172/15-1), the Grant-in-Aid for Scientific Research from JSPS (Grants No. 19201023 and No. 19681013) and IMS International Program, the Swedish Research Council, the C. Tryggers Foundation, and the Swedish National Infrastructure for Computing (SNIC).

*hildk@uni-mainz.de

[1] J. Stöhr, J. Magn. Magn. Mater. **200**, 470 (1999).
[2] B. T. Thole, P. Carra, F. Sette, and G. van der Laan, Phys. Rev. Lett. **68**, 1943 (1992).
[3] P. Carra, B. T. Thole, M. Altarelli, and X. Wang, Phys. Rev. Lett. **70**, 694 (1993).
[4] T. Nakagawa and T. Yokoyama, Phys. Rev. Lett. **96**, 237402 (2006).
[5] T. Nakagawa, T. Yokoyama, T. Hosaka, and M. Katoh, Rev. Sci. Instrum. **78**, 023907 (2007).
[6] K. Hild, J. Maul, T. Meng, M. Kallmayer, G. Schönhense, H. J. Elmers, R. Ramos, S. K. Arora, and I. V. Shvets, J. Phys. Condens. Matter **20**, 235218 (2008).
[7] K. Hild, J. Maul, G. Schönhense, H. J. Elmers, M. Amft, and P. M. Oppeneer, Phys. Rev. Lett. **102**, 057207 (2009).
[8] T. Nakagawa, I. Yamamoto, Y. Takagi, K. Watanabe, Y. Matsumoto, and T. Yokoyama, Phys. Rev. B **79**, 172404 (2009).
[9] K. Hild, J. Emmel, G. Schönhense, and H. J. Elmers, Phys. Rev. B **80**, 224426 (2009).
[10] K. Hild, G. Schönhense, H. J. Elmers, T. Nakagawa, T. Yokoyama, K. Tarafder, and P. M. Oppeneer, Phys. Rev. B **82**, 195430 (2010).
[11] G. K. L. Marx, H. J. Elmers, and G. Schönhense, Phys. Rev. Lett. **84**, 5888 (2000).
[12] G. Schönhense, H. J. Elmers, S. A. Nepijko, and C. M. Schneider, Adv. Imag. Elect. Phys. **142**, 159 (2006).
[13] A. Winkelmann, F. Bisio, R. Ocaña, W.-C. Lin, M. Nývlt, H. Petek, and J. Kirschner, Phys. Rev. Lett. **98**, 226601 (2007).
[14] A. Winkelmann, W.-C. Lin, C.-T. Chiang, F. Bisio, H. Petek, and J. Kirschner, Phys. Rev. B **80**, 155128 (2009).
[15] C.-T. Chiang, A. Winkelmann, P. Yu, J. Kirschner, and J. Henk, Phys. Rev. B **81**, 115130 (2010).
[16] T. Miller, W. E. Mc Mahon, and T. C. Chiang, Phys. Rev. Lett. **77**, 1167 (1996).
[17] S. R. Barman and K. Horn, Appl. Phys. A **69**, 519 (1999).
[18] S. R. Barman, C. Biswas, and K. Horn, Phys. Rev. B **69**, 045413 (2004).
[19] W. B. Zeper, F. J. A. M. Greidanus, P. F. Carcia, and C. R. Fincher, J. Appl. Phys. **65**, 4971 (1989).
[20] S. C. Shin, Appl. Surf. Sci. **65-66**, 110 (1993).
[21] N. W. E. Mc Gee, M. T. Johnson, J. J. de Vries, and J. van de Stegge, J. Appl. Phys. **73**, 3418 (1993).
[22] H. Schall, W. Huber, H. Hoermann, W. Maus-Friedrichs, and V. Kempter, Surf. Sci. **210**, 174 (1989).
[23] F. May, M. Tischer, D. Arvanitis, M. Russo, J. H. Dunn, H. Henneken, H. Wende, R. Chauvistré, N. Mårtensson, and K. Baberschke, Phys. Rev. B **53**, 1076 (1996).
[24] S. Pick and H. Dreyssé, Phys. Rev. B **59**, 4195 (1999).
[25] W.-C. Lin, A. Winkelmann, C.-T. Chiang, F. Bisio, and J. Kirschner, New J. Phys. **12**, 083022 (2010).
[26] R. Wu and A. J. Freeman, Phys. Rev. B **45**, 7532 (1992).
[27] S. H. Ma, Z. Y. Jiao, T. X. Wang, and Z. X. Yang, Eur. Phys. B **75**, 469 (2010).
[28] D. V. Chudinov, S. E. Kul'kova, and I. Yu. Smolin, Phys. Solid State **45**, 590 (2003).
[29] M. C. Xu, T. Iimori, K. D. Lee, and F. Komori, Surf. Sci. **505**, 243 (2002).
[30] M. Cinchetti, A. Oelsner, G. H. Fecher, H. J. Elmers, and G. Schönhense, Appl. Phys. Lett. **83**, 1503 (2003).
[31] P. M. Oppeneer, T. Maurer, J. Sticht, and J. Kübler, Phys. Rev. B **45**, 10924 (1992).